Optics Letters

Compressive motionless optical scanning holography

Qingyang Fu,[1,2] **Jiasong Sun,**[1,2] **Yaping Zhang,**[3] **Ting-Chung Poon,**[4] **Yao Fan,**[1,2,5] **and Chao Zuo**[1,2,*]

[1]*Smart Computational Imaging Laboratory (SCILab), School of Electronic and Optical Engineering, Nanjing University of Science and Technology, Nanjing, Jiangsu Province 210094, China*
[2]*Jiangsu Key Laboratory of Spectral Imaging & Intelligent Sense, Nanjing, Jiangsu Province 210094, China*
[3]*Yunnan Provincial Key Laboratory of Modern Information Optics, Kunming University of Science and Technology, Kunming, Yunnan 650500, China*
[4]*Bradley Department of Electrical and Computer Engineering, Virginia Tech, Blacksburg, Virginia 24061, USA*
[5]*fanyao@njust.edu.cn*
**zuochao@njust.edu.cn*

Received 13 January 2025; revised 26 February 2025; accepted 5 March 2025; posted 6 March 2025; published 1 April 2025

Optical scanning holography (OSH) is a powerful computational imaging technique that encodes three-dimensional (3D) information of an incoherently illuminated or self-luminous object into 2D holograms using Fresnel zone patterns (FZPs) as structured illumination. However, conventional OSH methods require complex setups with mechanical scanning or multi-frame phase-shifting devices, limiting their imaging efficiency and system stability. In this Letter, we propose compressive motionless optical scanning holography (CMOSH), a novel, to the best of our knowledge, framework that eliminates the need for phase shifting and mechanical scanning in 3D incoherent holography. The unique combination of compressive holography and motionless OSH enables single-scan, twin-image-free holographic reconstructions, significantly improving the system stability and imaging throughput. It also provides true 3D depth-resolved imaging, accurately resolving multi-layer samples while eliminating defocused information. The effectiveness of CMOSH is demonstrated through numerical simulations and experimental demonstrations, highlighting its potential for robust and efficient 3D holographic imaging across diverse applications.

https://doi.org/10.1364/OL.555692

Optical scanning holography (OSH) [1] is a computational imaging technique that encodes three-dimensional (3D) information of incoherent objects into two-dimensional (2D) holograms using Fresnel zone patterns (FZPs) as structured illumination. In contrast to methods such as Fresnel incoherent correlation holography (FINCH) [2] or off-axis holography [3] and phase-shifting holography [4], OSH achieves 3D imaging through a single-pixel detection approach. This capability has enabled OSH to be widely applied in fluorescence imaging [5], microscopic quantitative phase imaging [6,7], and remote sensing [8]. However, conventional OSH requires complex setups with phase-shifter [9], optical heterodyning [10], or mechanical scanning systems to achieve twin-image-free holograms. These configurations introduce stability challenges and limit imaging efficiency, particularly in dynamic or real-time applications.

To enhance the imaging efficiency of OSH, sub-sampling scanning techniques have been proposed to reduce the number of scans by using spiral scanning [11] or selectively omitting [12,13] some of the to-be-scanned information by measuring the correlation between scanned pixel points. These methods reduce acquisition time, but complex optical setups cannot prevent scanner vibrations from affecting the stability of the FZP. As an alternative, a heterodyne-free motionless optical scanning holography (MOSH) [14] solution has been proposed. MOSH is a highly stable variant of OSH that generates a FZP structured light via a spatial light modulator (SLM), which avoids the mechanical vibration of conventional OSH and provides a more simplified optical path, using four-step phase shifting (4PS) to acquire twin-image-free reconstruction. However, the 4PS still limits the acquisition time of MOSH. Naru *et al.* [15] subsequently proposed spatially divided phase-shifting MOSH (SP-MOSH) with 4PS FZPs arranged in interleaved rows to reduce the acquisition time. Without the use of heterodyning, off-axis FZP scanning of the object is used in off-axis OSH [16] to reconstruct the twin-image-free reconstruction through a single-frame hologram.

Compressed sensing (CS) [17] opens up a new way of solving the problem of signal acquisition and reconstruction in optical imaging technology. Brady *et al.* [18] modeled a Gabor hologram [19] as a sum of products of several discrete layers of an object and the corresponding measurement matrix based on the theory of CS achieving 3D tomography of the object using a single-frame 2D in-line Gabor hologram. Subsequently, Zhang *et al.* [20] used the CS framework for twin-image elimination for in-line digital holography of single-layer object. CS has also been applied to obtain artifact-free reconstruction by using a Fresnel zone aperture (FZA) camera with a single shot when the object is under incoherent illumination [21]. In addition, the feasibility of 2D random sparse sampling for computational OSH

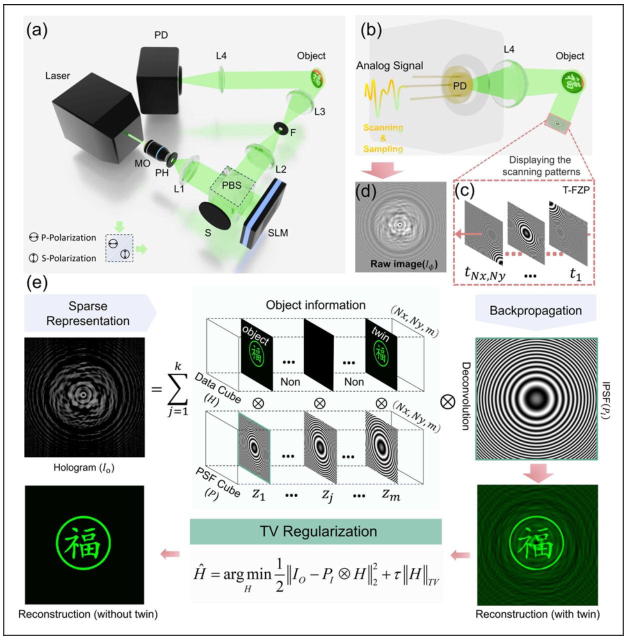

Fig. 1. Schematic diagram of the CMOSH optical system: (a) Reflective setup using a spatial light modulator (SLM) to generate Fresnel zone patterns (FZPs). (b) Enlarged view of the scanning configuration. (c) Shifted FZP projected during scanning. (d) Captured raw hologram. (e) Workflow of the CMOSH algorithm for twin-image and out-of-focus noise elimination. MO, microscope objective; PH, pinhole; L1–L4, lens; S, beam stopper; PBS, polarization beam splitter; F, filter.

hologram [22] has recently been discussed. This method breaks the limitations of traditional OSH spiral sparse scanning.

In this Letter, we propose a compressive MOSH (CMOSH) that achieves artifact-free reconstruction of object surface characteristics through sparse representation modeling of both target features and twin-image components in single-shot, phase-shift-free MOSH hologram. Through theoretical analysis, the collected light intensity compression information is considered as the convolution sum of the axial sparse object intensity containing twin-image artifacts and the measurement matrix. By combining the CS algorithm, the required signal can be effectively decompressed without loss, thus achieving clearer holographic reconstruction without twin-image artifacts compared to traditional 4PS methods. We further demonstrate the depth-resolving capability of CMOSH, enabling the acquisition of a clear, focused layer-specific image from a single frame, without interference from other unfocused layers.

The CMOSH system employs a reflective optical setup, as illustrated in Fig. 1(a). The light emitted by the laser is focused by a microscope objective (MO) and filtered through a pinhole (PH) to give a collimated optical beam by lens L1. The beam first passes through a polarization beam splitter (PBS), the transmitted light is modulated into p-polarized light and part of it is modulated by a SLM through birefringence polarization characteristics into a modulated wavefront and an unmodulated wavefront. After filtering out unwanted multi-order terms via a $4f$ system consisting of lenses L2 and L3 (Fig. 1(b)), interference occurs to generate FZPs as scanning patterns for structured illumination. The reflected light, encoded with the object information, is collected by photodetector (PD), which gives an analogy signal for processing. The MOSH system is in an incoherent mode; it can only obtain a current I_ϕ from the PD that is proportional to the intensity convolution of a certain determined FZP to the sample:

$$I_\phi(x,y) \propto \int_z O(x,y;z) \otimes FZP_\phi(x,y;z)dz, \tag{1}$$

where $O(x,y;z)$ is the reflectivity of the object surface. $\otimes$ denotes the convolution operation, and $FZP_\phi = 1 + cos[k/2z(x^2+y^2)+\phi]$ with ϕ denoting phase shift. $I_\phi(x,y)$ contains a DC component and two mutually conjugate twin images, which are equivalent to Gabor in-line hologram. Usually, optical heterodyne [10], multi-step phase shifting [7,14], or off-axis FZP [16] are required to get more data to separate twins and remove the DC component. CS enables single-shot MOSH to remove undesired out-of-focus artifacts as well as the twin image. We consider the object image is sparse, and valid information exists only in the m discrete layers in the z-direction. Assuming that the sampling number of the 2D signals acquired by the PD is $N_x \times N_y$, the point spread function (PSF) of the light field propagation can be regarded as the measurement matrix $P_{(N_x \times N_y \times m)}$ in acquiring the observation information, which is a collection of DC-free FZP_ϕ located at different depths z_j. During CS reconstruction, DC components that do not contribute to the valid information are usually removed to obtain hologram I_o; i.e., I_o=I_ϕ-$\overline{I_\phi}$, and $\overline{I_\phi}$ is the average of I_ϕ. The DC-free hologram $I_{o(N_x \times N_y)}$ can be regarded as the convolution sum of the m layers object information $H_{(N_x \times N_y \times m)}$ and the corresponding depth measurement matrix, which can be represented as an m-sparse signal:

$$I_{o(N_x \times N_y)} = \sum_{j=1}^{m} P_{(N_x \times N_y; z_j)} \otimes H_{(N_x \times N_y; z_j)}. \tag{2}$$

As illustrated in Fig. 1(e), I_o obtained from single scanning which can be modeled as the convolution sum of a 3D PSF cube $P_{(N_x \times N_y; z_j)}$ and data cube $H_{(N_x \times N_y; z_j)}$. Inverse PSF (IPSF) is the complex conjugate of PSF at the corresponding z-direction, i.e., $P_{I(N_x \times N_y; z_j)}$=$\exp(-jk\sqrt{x(N_x)^2 + y(N_y)^2 + z_j})$. It can be regarded as the sensing matrix used in reconstructing the object information. Since I_o contains multi-layers of information, direct convolution of the IPSF measurement matrix for backpropagation (BP) will cause the twin image, that interferes with the focused reconstructed image. Therefore, we use a CS method to eliminate the twin-image noise and the out-of-focus noise on the reconstructed image. Due to the energy conservation property of both PSF and IPSF, the raw hologram before and after BP and the reconstruction result remain energy-conserving. Thus, so the measurement matrix $P_{(N_x \times N_y; z_j)}$ and the sensing matrix $P_{I(N_x \times N_y; z_j)}$ satisfy the restricted isometry property (RIP) [23,24]. The object information is modeled as an underdetermined minimum value optimization problem and can be solved iteratively by the TV regularization:

$$\widehat{H} = \underset{H}{argmin}\, \frac{1}{2}\|I_o - P_I \otimes H\|_2^2 + \tau\|H\|_{TV}, \tag{3}$$

where τ denotes the regularization parameter, $\|.\|_2$ is the L_2 norm operator, and $\|.\|_{TV}$ denotes the total variation operator. By using the above steps, the object information can be maximally preserved, and the twin-image and the out-of-focus noise can be removed by a single hologram. In addition, if I_o contains more than two layers of information, it is also possible to perform

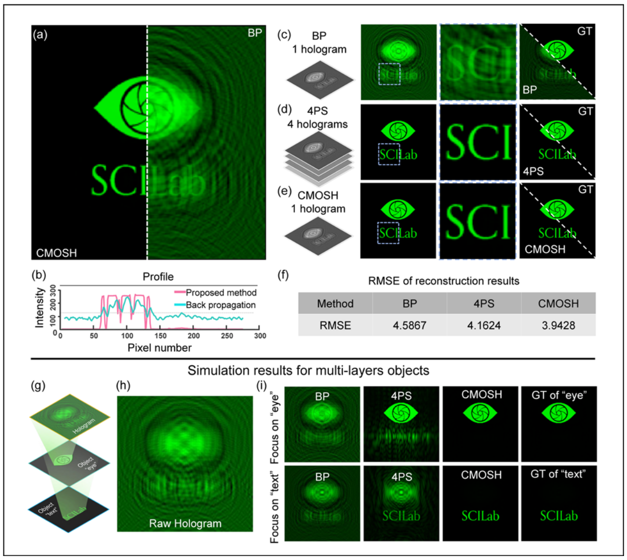

Fig. 2. Comparison of reconstruction methods: BP, 4PS, and CMOSH. (a) CMOSH result (left panel) and direct backpropagation (BP) result (right panel) with a single MOSH hologram. (b) Cross section of the reconstruction result in (a). (c)–(e) MOSH capture images and the reconstruction results under BP, 4PS, and CMOSH schemes and the corresponding GT. (f) RMSE of reconstruction results. (g) Schematic of a multi-layer object with a hologram. (h) Raw hologram of a multi-layer object from single scanning. (i) Multi-layer object reconstruction from BP, 4PS, and CMOSH.

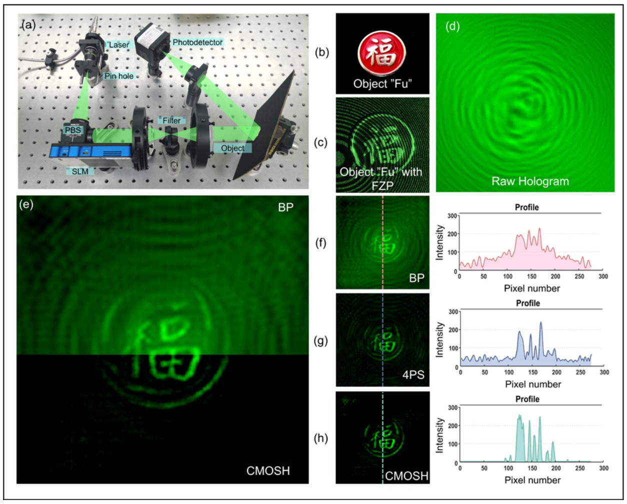

Fig. 3. Experimental validation of CMOSH with a single-layer object: (a) Optical setup of the CMOSH system. (b) Metal badge "Fu" used as the test object. (c) Captured FZP pattern with the object. (d) Raw single hologram. (e) Comparison of reconstruction results using BP and CMOSH methods, highlighting twin-image suppression. (f)–(h) Comparison of the reconstruction results using the BP, 4PS, and CMOSH methods and their corresponding profile lines along the dashed lines.

CS reconstruction of objects with different depths by means of different depths of measurement matrices. As a result, the CMOSH method can remove the twin image of individual object and also has the ability to perform sectioning in different planes using a 2D single hologram. In CMOSH, we use the two-step iterative shrinkage/thresholding (TwIST) [25] to solve the TV regularization problem in Eq. (3).

In order to verify the effectiveness of the CMOSH, the reconstructed results under different methods are compared by numerical simulations, which include 4PS, BP, and CMOSH reconstruction. Specifically, FZP_0 is used to obtain a single hologram, and 4PS captures four holograms by FZP_0, $FZP_{\frac{\pi}{2}}$, FZP_{π}, and $FZP_{\frac{3\pi}{2}}$. The full-field comparison of BP and CMOSH is shown in Fig. 2(a). In contrast, the CMOSH reconstruction results have almost no twin-image and out-of-focus artifacts. Figures 2(c)–2(e) display the simulation results. From Fig. 2(h), it can be seen that the direct BP method using a single hologram fails to separate the object image and the twin image, with very obvious out-of-focus artifacts. The 4PS method using four holograms yields a clear image of the focused object, but out-of-focus noise remains. The CMOSH scheme using a single hologram remove the twin-image as well as the out-of-focus noise to obtain a clear focused object image. We further use the root mean square error (RMSE) to quantitatively measure the error of the reconstructed results from the ground truth (GT). In Fig. 2(f), the RMSE metrics indicate that there is a significant difference between the direct BP and GT; however, the 4PS results are almost indistinguishable from the GT, and the RMSE decreases by 9.25% compared to the direct BP. In contrast, the CMOSH reconstruction results in the smallest RMSE, which is further reduced by 5.28% compared to the 4PS. This means that although only a single hologram is needed, CMOSH obtains reconstruction results that are much closer to the GT.

When dealing with multi-layer objects, single-layer reconstruction methods typically struggle with interference from out-of-focus images and twin-image artifacts originating from different layers. In order to evaluate the imaging capability of CMOSH for multi-layer objects, we further demonstrate its layer to reso capability on depth for multi-layer objects by simulation. Figures 2(g)–2(i) give the 4PS and CMOSH experimental results. Although the 4PS method is good at eliminating a twin image, but it does not eliminate out-of focus noise of multi-layer object. By comparison, CMOSH can obtain reconstructed results without out-of- focus artifacts for each layer of multi-layer objects. This result proves that CMOSH not only is capable of obtaining twin-image-free reconstruction from a single hologram but also possesses layer resolve capability.

We further demonstrated the capabilities of the CMOSH method in an actual experimental setup, as shown in Fig. 3(a). The system employed a 532 nm semiconductor laser (ASML JDSU 21012386, 21011871-001) coupled to a pinhole filter (Thorlabs P50CB) via single-mode fibers to produce a quasi-spherical wave for collimation by a lens. The SLM (Casmicrostar FSLM-2K70-A02) is capable of both amplitude and phase modulation. The light reflected from the SLM displaying FZPs illuminates the object and is subsequently captured by a PD (Lubang PD-SAF-3201-20K). The analog signal from the PD was converted into a digital signal using an analog-to-digital converter (ADC, Arduino UNO R4). The digital data is then stored on a computer for processing. The single-scanned hologram consists of 270×270 sampling points. The object and the FZP pattern overlapping with the object in the optical experiment are depicted in Figs. 3(b) and 3(c), respectively.

Figure 3(d) shows the raw hologram. Due to the limitation of the refresh rate of the SLM, the acquisition cost for a single hologram is approximately 25 min. As shown in Fig. 3(e), our

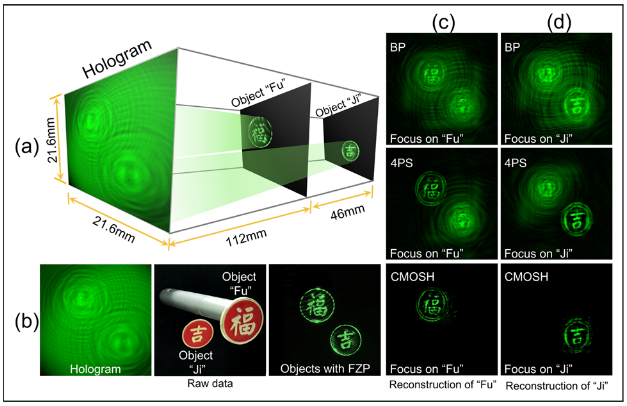

Fig. 4. Multi-layer object reconstruction. (a) Setup of the multi-layer objects "Fu" and "Ji" placed at different axial depths. (b) Captured single hologram. (c) Reconstructed image of object "Fu" using BP, 4PS, and CMOSH. (d) Reconstructed image of object "Ji" showing superior twin-image suppression and out-of-focus noise elimination with CMOSH.

CMOSH method achieves reconstruction results (lower panel) free from twin-image artifacts using a single hologram as compared to the result using BP (top panel). The reconstruction were performed on an Intel Core i5-14490F processor operating at 2.80 GHz, the time cost of 0.3s for BP/4PS and 10s for CS, respectively. In contrast, Figs. 3(f)–3(h) reveal that the reconstructed results free from BP and 4PS methods exhibit visible noise and artifacts due to the effects of twin-image interference and noise terms. Notably, the optical experimental reconstruction results of the proposed CMOSH method display minimal unanticipated noise artifacts, which are nearly unobservable. This demonstrates the capability of CMOSH to effectively eliminate the influence of twin-image artifacts on the reconstructed result while avoiding additional noise introduced by multi-scanning procedures. Cross-sectional plots corresponding to the three methods provide intuitive evidence supporting this conclusion.

We also performed experiments with two metal badges labeled "Fu" and "Ji" placed at distinct axial depths (Fig. 4(a)). The hologram captured during a single scan (Fig. 4(b)) was processed using CMOSH, BP, and 4PS methods. As shown in Figs. 4(c) and 4(d), BP failed to suppress twin-image artifacts, leading to severe cross-layer interference. The 4PS method partially mitigated these effects but could not eliminate out-of-focus noise. In contrast, CMOSH effectively separated the layers, achieving clear reconstructions of both objects without cross-layer interference. Experimental results demonstrate that CMOSH achieves layer-resolved artifact-free reconstructions using a single hologram. In comparison, methods such as BP and 4PS exhibit prominent twin-image or out-of-focus artifacts in their reconstructed outputs. For a video demonstration of the optical setup and processing, please refer to Visualization 1.

We represent the CMOSH hologram as axially sparse intensity superposition as compressed information and achieve decompression of multi-layer objects through IPSF sensing matrix deconvolution and CS algorithm. The theoretical model conforms to the RIP principle and provides a theoretical basis for the development of the CMOSH compression framework in the future. The validity of this model is proved by the twin-image-free reconstruction of numerical simulation and optical experiments, which is expected to provide an effective technical solution for the detection of object surface characteristics. However, its performance may degrade for densely distributed multi-layer objects, as the layer-resolving capability relies on the axial sparsity assumption. The numerical simulation results also indicate that as the amount of object information increases, the layer resolve performance decreases (see Supplement 1 for specific analysis), but improving the resolution of holograms has a positive effect on overcoming this phenomenon. Future research will focus on enhancing the robustness of CMOSH by integrating advanced sparsity priors or deep learning based reconstruction algorithms.

Funding. National Natural Science Foundation of China (62305162, U21B2033, 62227818, 62361136588, 62275113); Nanjing University of Science and Technology (AE891548); National Key Research and Development Program of China (2022YFA1205002, 2024YFE0101300); Biomedical Competition Foundation of Jiangsu Province (BE2022847); Fundamental Research Funds for the Central Universities (30923010206, 2023102001); Open Research Fund of Jiangsu Key Laboratory of Spectral Imaging & Intelligent Sense (JSGP202105, JSGP202201).

Disclosures. The authors declare no conflicts of interest.

Data availability. Data underlying the results presented in this Letter are not publicly available but may be obtained from the authors upon reasonable request.

Supplemental document. See Supplement 1 for supporting content.

REFERENCES

1. T.-C. Poon, *Optical Scanning Holography with MATLAB* (Springer, 2010).
2. J. Rosen and G. Brooker, Opt. Lett. **32**, 912 (2007).
3. J. Zhang, S. Dai, C. Ma, *et al.*, Light: Adv. Manuf. **10**, 23 (2021).
4. I. Yamaguchi and T. Zhang, Opt. Lett. **22**, 1268 (1997).
5. G. Indebetouw and W. Zhong, J. Opt. Soc. Am. A **23**, 1699 (2006).
6. G. Indebetouw, Y. Tada, and J. Leacock, BioMed. Eng. OnLine **5**, 63 (2006).
7. N. Yoneda, O. Matoba, Y. Saita, *et al.*, Opt. Lett. **48**, 5273 (2023).
8. B. W. Schilling and G. C. Templeton, Appl. Opt. **2**, 476 (2001).
9. J. Rosen, G. Indebetouw, and G. Brooker, Opt. Express **14**, 4280 (2006).
10. T.-C. Poon, J. Opt. Soc. Am. A **2**, 521 (1985).
11. A. C. Chan, K. K. Tsia, and E. Y. Lam, Optica **3**, 911 (2016).
12. P. W. Tsang, J.-P. Liu, and T.-C. Poon, Optica **2**, 476 (2015).
13. P. Tsang, T.-C. Poon, and J.-P. Liu, Sci. Rep. **6**, 21636 (2016).
14. N. Yoneda, Y. Saita, and T. Nomura, Opt. Lett. **45**, 3184 (2020).
15. N. Yoneda, Y. Saita, and T. Nomura, OSA Continuum **3**, 3523 (2020).
16. Y. Zhang, Y. Yao, J. Zhang, *et al.*, J. Opt. Soc. Am. A **39**, A44 (2022).
17. D. L. Donoho, IEEE Trans. Inf. Theory **52**, 1289 (2006).
18. D. J. Brady, K. Choi, D. L. Marks, *et al.*, Opt. Express **17**, 13040 (2009).
19. D. Gabor, Nature **161**, 777 (1948).
20. W. Zhang, L. Cao, D. J. Brady, *et al.*, Phys. Rev. Lett. **121**, 093902 (2018).
21. J. Wu, H. Zhang, W. Zhang, *et al.*, Light: Sci. Appl. **9**, 53 (2020).
22. N. Yoneda, M. Sugimoto, Y. Saita, *et al.*, Appl. Opt. **64**, B102 (2025).
23. E. J. Candès, J. K. Romberg, and T. Tao, Commun. Pure Appl. Math. **59**, 1207 (2005).
24. E. J. Candès and T. Tao, IEEE Trans. Inf. Theory **52**, 5406 (2006).
25. J. M. Bioucas-Dias and M. A. T. Figueiredo, IEEE Trans. on Image Process **16**, 2992 (2007).